E-Journal of Advanced Maintenance Vol.7-2 (2015) 172-178
Japan Society of Maintenology

Non-Destructive Evaluation of Multiple-site Small Cracks in Low Cycle Fatigue of Austenitic Stainless Steel by Four-point Probe DC Potential Difference Method

Shio NAKANISHI[1,*], Takayuki SUZUKI[2] and Yuji NAKASONE[1]

[1] *Tokyo University of Science, 6-3-1 Niijuku, Katsushika-ku, Tokyo 125-8585, Japan*
[2] *National Institute of Advanced Industrial Science and Technology, 1-2-1 Namiki, Tsukuba-shi, Ibaraki 305-8564, Japan*

ABSTRACT

This study has investigated multiple-site small cracks in the low cycle fatigue of SUS316L at 873K in air by using the four-point probe DC potential difference method. Small probes with 1-mm spacing between the electrodes were used in order to evaluate small cracks of some hundred micrometers. Morphology of the cracks was evaluated by standard deviation of potential difference σ_V which detected by the probes and by the crack density by laser microscopy. As a result, it was shown that σ_V monotonically increased with increasing number of strain cycles and fatigue process was classified into four stages. Furthermore, statistical analysis showed that the cracks initiated at random sites in early stage. However, the randomness was diminished and σ_V increased significantly with growth and coalescence of the cracks. These results revealed that standard deviation of normalized potential difference could evaluate initiation, growth and coalescence of multiple-site small cracks in each stage.

KEYWORDS

Low cycle fatigue, Austenitic stainless steel, Multiple-site small cracks, Crack growth and coalescence, Four-point probe DC potential difference method, Statistical analysis

ARTICLE INFORMATION

Article history:
Received 2 December 2014
Accepted 3 July 2015

1. Introduction

Recently, in power plants, Condition-Based Maintenance (CBM) is required instead of Time-Based Maintenance (TBM) in order to improve the safety and dependability of the plants. Especially, on surfaces of structural components of the power plants, multiple-site small cracks initiate, grow and coalesce due to high-temperature low cycle fatigue, and they finally form larger cracks which cause fracture. In order to ensure the integrity of these power plants by CBM, it is necessary to detect multiple-site small cracks growth and to predict fatigue life of structural parts nondestructively.

DC/AC potential difference method can detect potential difference distribution around a single crack/cracks and was applied to identify dimensions of a single large crack in previous studies [1, 2, 3]. A few researches [4, 5] reported variation in potential difference of multiple-site small cracks. However, the relationship between changes in potential difference and behavior of multiple-site small cracks has not yet been investigated. The present authors have applied the four-point probe DC potential difference method to the non-destructive evaluation of multiple small cracks in high-temperature low cycle fatigue of an austenitic stainless steel JIS SUS316L. In each stage of the fatigue process, DC potential difference on specimen surfaces, and density and sizes of multiple-site small cracks in specimens were measured and statistically analyzed [6, 7]. This paper describes the statistical analysis of the growth behavior of multiple-site small cracks and the prediction of residual life of the fatigue process by using four-point probe DC potential difference method.

2. Experimental procedures

*Corresponding author, E-mail: 4513636@ed.tus.ac.jp

2.1. High-temperature low cycle fatigue tests

Figure 1 shows the geometry of specimens made of an austenitic stainless steel JIS SUS316L, equivalent of AISI Type 316L. The chemical composition of the steel was shown in Table 1. Low cycle fatigue tests were carried out at 873K in air under completely reversed tension and compression strain control. A total strain range of $\Delta\varepsilon_t$=1.5% was applied to specimens at a strain rate of 0.1%/sec. An extensometer composed of two heat-resistant rods of a gage length of 12 mm were used to measure strain and to control the strain range to be applied to each specimen tested. Fatigue tests were interrupted and resumed repeatedly at adequate intervals until the fracture of specimens, or the time at which the maximum tensile stress decreased by 25% of the steady-state peak stress following the high-temperature low-cycle fatigue test method provided by JIS Z 2279-1992.

2.2. Four-point probe DC potential difference method

Potential difference was measured by DC potential difference measuring system which consists of four-point microprobe, controller (Denshijiki Industry Co., Ltd. WT-4102), X-Y automatic stage and data-collection PC. Figure 2 shows the schematic diagram of four-point microprobe with 1-mm spacing between the electrodes. A pair of outermost electrodes supplies DC current, and the other pair of inner electrodes measures potential difference produced. Since the electrodes and their interval are small, this system can measure local potential difference which changes due to the initiation and growth of multiple small cracks. During the stop time of fatigue tests, specimen surfaces were buffed first with alumina suspension to remove oxide layer, then the four-point probe scanned specimen surfaces at a step size of 0.5 mm in the longitudinal direction x and that of 1.4 mm in the circumferential direction θ. Figure 3 schematically illustrates the present measurement area of 10 mm in the longitudinal direction by 9.8 mm, or 140 degrees in the circumferential direction. The length of the measurement area in the radial direction was set to 140 degrees, because cement that prevented extensometer slip during fatigue tests was applied to the remaining specimen surface. The

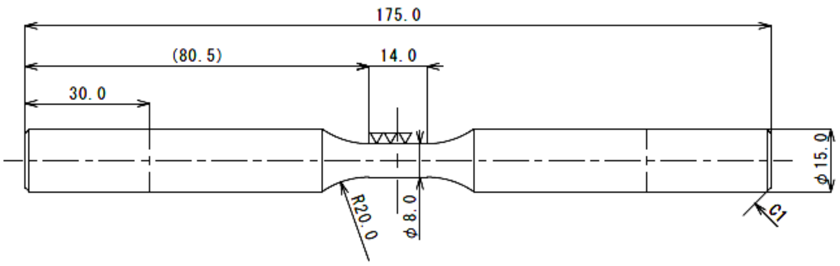

Fig. 1 Geometry of specimens (unit: mm).

Table 1 Chemical composition of the present austenitic stainless steel SUS316L (wt%).

C	Si	Mn	P	S	Ni	Cr	Mo
0.019	0.39	0.81	0.028	0.001	12.00	17.59	2.1

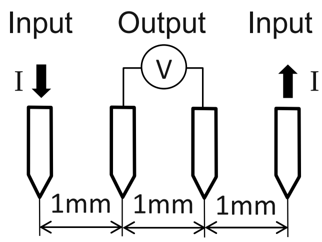

Fig.2 Schematic illustration of four-point microprobe.

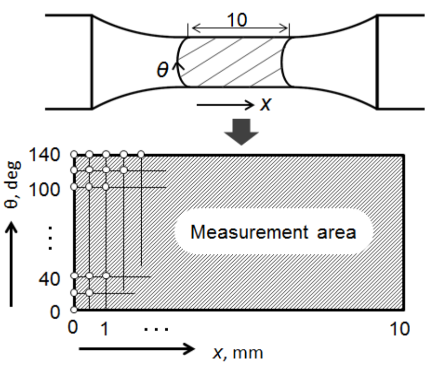

Fig. 3 Measurement area for potential difference, and crack density and sizes.

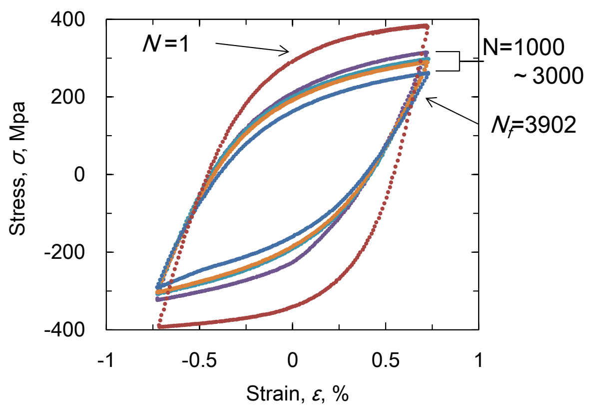

Fig. 4 Variations in stress-strain curves during high-temperature low cycle fatigue of SUS316L.

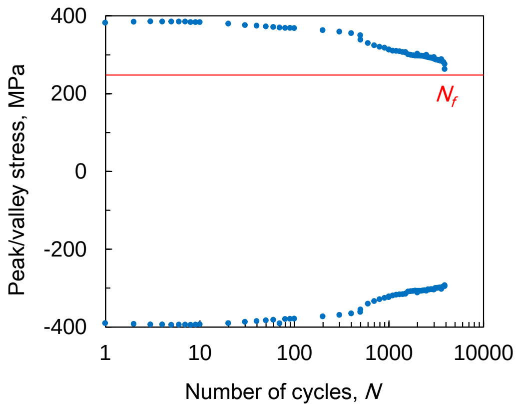

Fig. 5 Time variation of peak/valley stresses during high-temperature low cycle fatigue of SUS316L.

measurement area covers about 40 % of the specimen surface, and enough number of cracks were observed to determine statistical distributions of cracks and those of potential differences in the specimen. The total number of measured points was 168 for each specimen inspected. The DC electric current applied was 0.4 A or 0.8 A.

2.3. Crack density

The densities of multiple-site small cracks were measured by scanning laser microscopy during the stop time of fatigue tests. Crack density ρ at a point (x, θ) on a specimen surface was defined as the number of cracks crossing a longitudinal line segment of 1 mm with the point (x, θ) placed at the center of the line segment connecting points (x-0.5, θ) and (x+0.5, θ).

3. Results and discussion

3.1. High-temperature low cycle fatigue tests

Figure 4 shows an example of stress-strain curves observed in the present high-temperature low cycle fatigue tests. Figure 5 shows a relationship between peak/valley stresses and number of strain cycles N. Peak/valley stresses decreased gradually with increasing N and abruptly decreased just before final fracture. Figure 6 shows the photomicrographs of surface changes of the specimens tested. Crack initiations were observed after N/N_f=0.26. At N/N_f=0.38~0.90, additional crack initiations were scarcely observed, whereas crack growth accompanied by coalescence with other cracks were frequently observed. Finally, a main crack was formed to cause fracture of specimens at N/N_f=1.

3.2. Crack density

Figures 7 (a) through (c) show examples of histograms of crack density ρ. The solid lines in the figures indicate theoretical Poisson distributions Po(ρ_a) calculated by using the mean crack density ρ_a. The value of ρ_a increased with increasing number of strain cycles, and the values of ρ_a at N/N_f=0.38～1 were larger than that at N/N_f=0.26. Figures 6 (b) and (c), however, reveal virtually no additional crack initiation at N/N_f=0.38~1. These observations indicate that the increase of the mean crack density ρ_a at $N/N_f \geqq 0.38$ was mainly due to the growth and coalescence of the cracks.

The χ^2 goodness-of-fit tests reveal that crack density ρ was regarded to follow a Poisson distribution at a significance level of α=10% at N/N_f=0.26. At N/N_f=0.38~0.9, however, the significance level at which the crack density was regarded to follow Poisson distributions decreased down to α=0.1%, and increased a little to α=5% at N/N_f=1. These results imply that cracks initiated independently of one another at random sites at N/N_f=0.26, whereas that, at $N/N_f \geqq 0.38$, additional cracks scarcely initiated and the existing cracks grew and coalesced with one another so that the

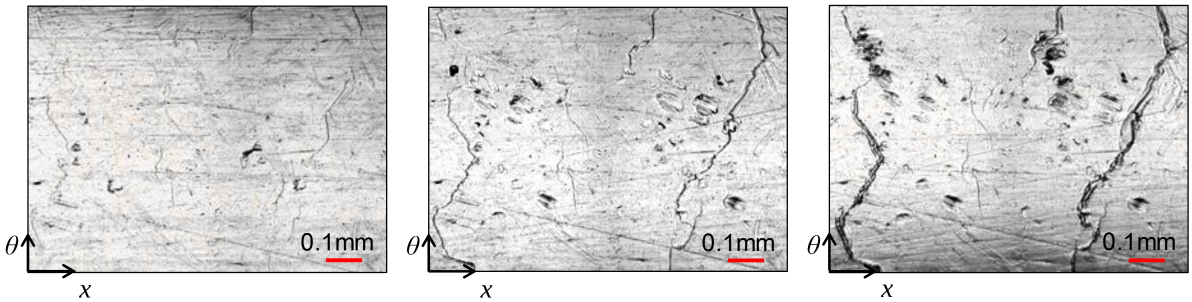

(a) N/N_f=0.26 (b) N/N_f=0.64 (c) N/N_f=1

Fig. 6 Laser photomicrographs showing surface change during high-temperature fatigue of SUS 316L.

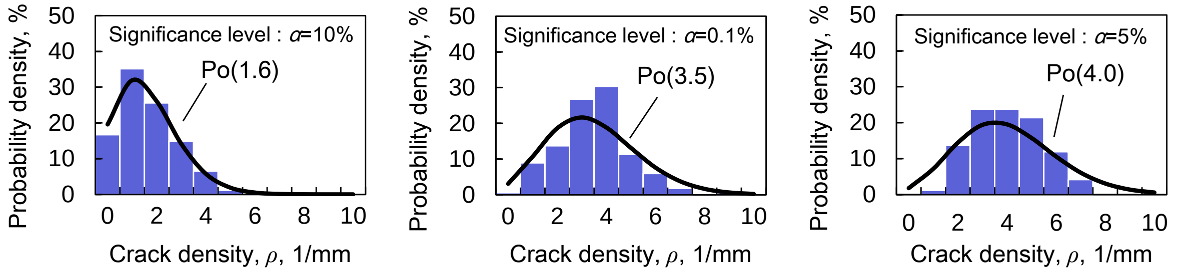

(a) N/N_f=0.26 (b) N/N_f=0.64 (c) N/N_f=1

Fig. 7 Variations in histograms of crack density during high-temperature fatigue of SUS 316L.

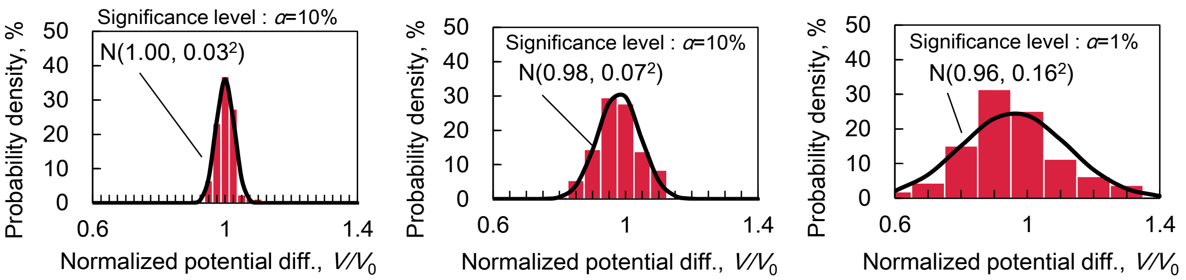

(a) N/N_f=0.26 (b) N/N_f=0.64 (c) N/N_f=1

Fig. 8 Variations in histograms of normalized potential difference during high-temperature fatigue of SUS 316L (I=0.8 A).

degree of the randomness in the crack sites was reduced.

The crack density ρ defined in the present paper depends not only on the number of cracks but on their surface lengths. Even if cracks grow without change in the number of the cracks, the crack density can increase. The crack density defined in this paper can be affected by the initiation and growth of cracks.

3.3. Potential difference

Figures 8 (a) through (c) show examples of histograms of normalized potential difference V/V_0 obtained at I=0.8A, where V_0 is average potential difference measured before the fatigue test of each specimen. The solid lines in the figures indicate theoretical normal distributions N(μ_a, σ_V^2) calculated by using the mean μ_a and the standard deviation σ_V of V/V_0. In early stage of fatigue, the value of V/V_0 varied very little, and varied widely with increasing N/N_f. At N/N_f=0～0.90, the normalized potential difference V/V_0 was regarded to follow normal distributions at a significance level of α=10%. At fracture, i.e., N/N_f=1, V/V_0 was regarded to follow a normal distribution at α=1%. Measurements of the potential difference were made at I=0.4A in some of the specimens tested, and almost the same results for the statistical distributions of V/V_0 were obtained.

The value of σ_V increased with increasing number of strain cycles, whereas the value of μ_a remained almost a constant value of 1.0 throughout the entire life cycle. These results imply that the

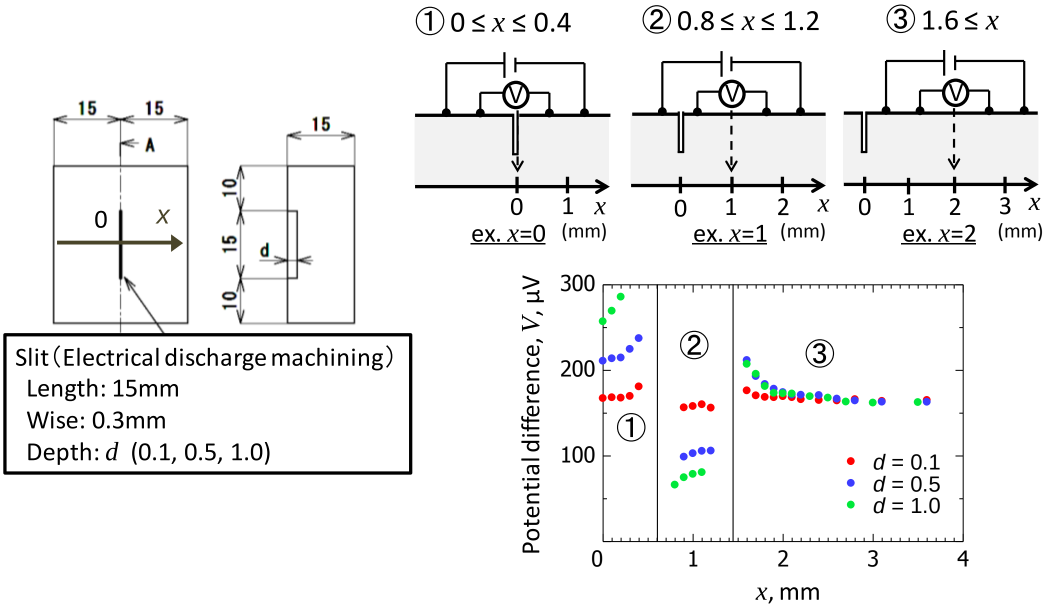

Fig. 9 Variation of potential difference across an artificial single surface crack with the relative position of the four-point probe to the crack: the figure shows the right half of the variation profile, since the variation is symmetric with respect to the origin of the local coordinate, i.e., x=0.

variation of σ_V characterizes the statistical distributions of V/V_0 which reflect the growth behavior of multiple-site small cracks.

Figure 9 shows the right half of the variation of potential difference across an artificial surface crack, which is symmetric with respect to the origin of the local coordinate, i.e., x=0, with the relative position of the four-point probe to the crack. In the cases where a pair of inner voltage measuring needles of the probe stride over the crack, the potential difference V increases drastically as one of the needles approaches to the crack flank (region ①). The potential difference V also increases drastically as one of the outer current supplying needles approaches to the crack when the probe moves away from the crack (region ③). In the case where a current supplying needle and a voltage measuring needle are placed on either side of the crack (region ②), the potential difference measured here is lower than the remote potential difference value V_0, which is equal to the average potential difference measured before the fatigue test of the specimen. For a shallow crack, the variation in the potential difference across the crack is so small that the potential difference value V remains almost its remote value V_0 across the crack. As a crack grows in surface length and in depth, the excess value of V increases in regions ① and ③, whereas the reduced value of V decreases in region ②. The regions of the excess potential difference becomes wider as the crack grows. In early stages of the present fatigue processes, when cracks were small both in surface length and in depth, the values of the potential difference measured by the multipoint microprobes did not vary so much around the value of the remote potential difference V_0. In later stages of the fatigue processes, the sizes of the cracks differ greatly due to the power-law growth and the accelerated growth by coalescence with other cracks so that the values of V vary so much around V_0 and the variance of V/V_0 becomes larger.

Figures 10 (a) and (b) depict photomicrographs of multiple-site small cracks observed on the longitudinal sections of specimens interrupted at N=2000 and fractured at N_f=5432, respectively. Figures 11 (a) and (b) show crack depths measured at different longitudinal positions by using photogrammetry procedures. Crack depth measured on the longitudinal sections in the interrupted specimen ranged from 0.009 to 0.110 mm, whereas that in the fractured specimen from 0.012 to 1.910 mm. Figures 11 (a) and (b) demonstrate that most of the cracks measured were larger in the fractured specimen than in the interrupted specimen.

3.4. Prediction of residual fatigue life

Figure 12 shows the variations in standard deviation of the normalized potential difference V/V_0,

σ_V, obtained at I=0.4 and 0.8A, and average crack density ρ_a with increasing N/N_f. The rate of increase in ρ_a was high in the initial stage of fatigue and gradually lowered in the latter stage, since crack growth accompanied with coalescence was predominant in the latter stage of fatigue. The rate of increase in σ_V, however, became higher with increasing number of strain cycles and exhibited marked increase at the last stage of fatigue, i.e., $N/N_f \geqq 0.9$ due to the accelerated growth of the main crack. Figure 12 implies that the present fatigue process in which multiple-site small cracks were involved can be divided into four stages; i.e., Stage I (incubation stage), Stage II (initiation stage), Stage III (growth and coalescence stage) and Stage IV (accelerated growth stage). Stages I and II cannot be clearly distinguished by the V/V_0 vs. N/N_f curve but by the ρ_0 vs. N/N_f curve. The incubation time for crack initiation during which no crack initiation was expected to occur was found as $N/N_f \fallingdotseq 0.12$, because the crack density remained zero until the N/N_f value reached approximately 0.12. Stages II and III were divided according to the laser photo-micrographic observation that cracks started

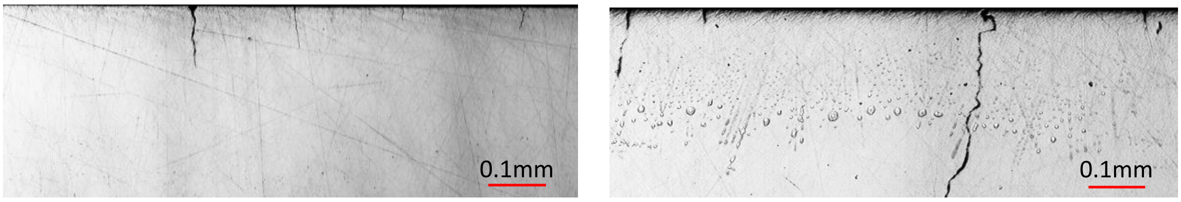

(a) N=2000 (interrupted) **(b) N_f=5432 (fractured)**

Fig. 10 Laser photomicrographs of cracks observed on the longitudinal sections of two specimens; one was interrupted at N=2000 and the other fractured at N=5432.

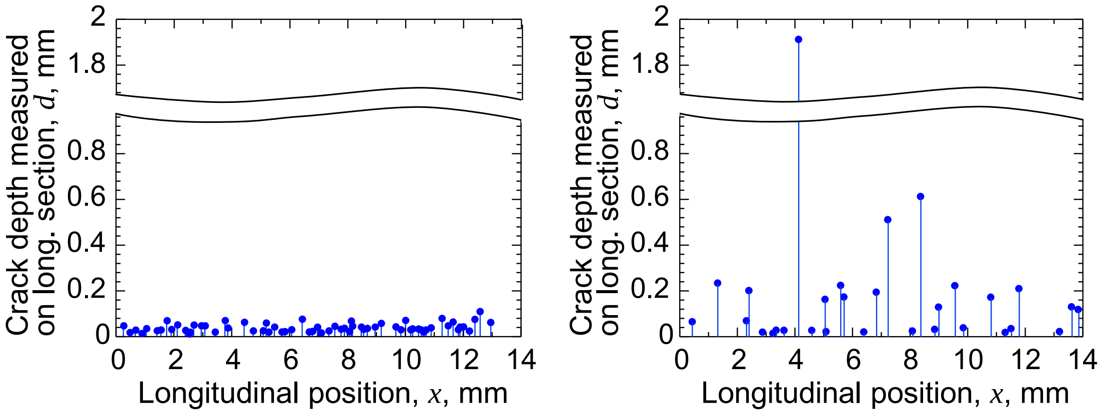

(a) N=2000 (interrupted) **(b) N_f=5432 (fractured)**

Fig. 11 Distributions of crack depths measured in the longitudinal sections of the two specimens shown in Fig. 10.

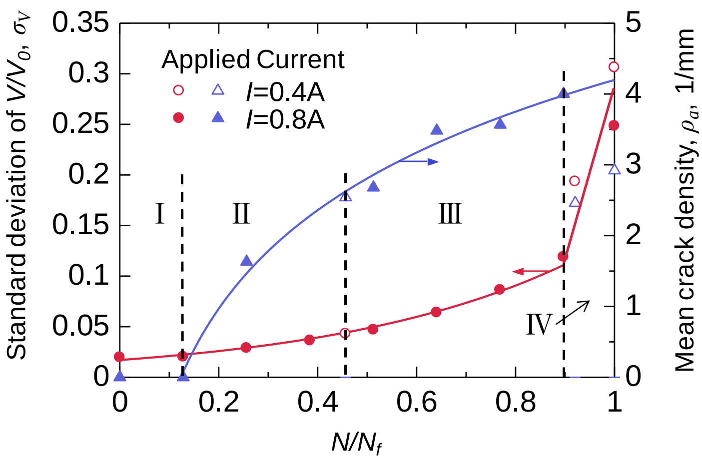

Fig. 12 Variations in standard deviation of the normalized potential difference V/V_0, σ_V, and the average crack density ρ_a indicating that the present fatigue process can be divided into four stages.

coalescing with one another.

The detection of the onset of the final Stage IV by four-point probe DC potential difference method can non-destructively predict the residual life of fatigue in which multiple-site small cracks are involved. Fig.12 suggests that the residual life prediction can be made at $N/N_f \fallingdotseq 0.9$ which corresponds to 390 to 810 cycles, or to the actual time duration of 3 to 6 hours. For actual structures or machines, the time duration corresponding to 10 % of fatigue life is much longer so that there is enough time left to take countermeasures against fatigue fracture according to the prediction made by the present method.

4. Conclusion

(1) Multiple-site small cracks initiated on the surfaces of specimens due to high-temperature low cycle fatigue, and the sizes of the small cracks varied with the number of strain cycles according to their growth and coalescence.

(2) Higher growth rate of larger cracks widened the size difference among multiple-site cracks to bring about much larger variation in local potential difference in the latter stage of the fatigue process.

(3) The detection of the onset of the final Stage IV by four-point probe DC potential difference method can non-destructively predict the residual life of fatigue in which multiple-site small cracks are involved.

Acknowledgement

The authors would like to express their gratitude to Mr. M. Iwata at R&D Department, Denshijiki Industry Co., Ltd. for his assistance for the four-point probe DC potential difference measurement.

References

[1] F. Takeo, N. Tada: "Progress in NDE Technologies for Crack Sizing by DC Potential Difference Method", , Journal of the Japan Society for Non-Destructive Inspection , Vol.60, No.10, pp.572-578 (2011).

[2] H. Tohmyoh, "Sensitive NDE of a Shallow Surface Crack Utilizing Surface Potential Drop Distribution", J. Journal of the Japan Society for Non-Destructive Inspection, Vol.57, No.5, pp.236-239 (2008).

[3] H. Kim, T. Shoji: "A Study on Induced Current Focusing Potential Drop (ICFPD) Technique-Examination of the Sizing Accuracy of Defects and Its Frequency Dependence", Journal of the Society of Materials Science, Japan, Vo;.43, No.494, pp.1482-1488 (1994).

[4] T. Shoji, T. Kawahara, M. Awano, Y. Sato: "Development of Nondestructive Evaluation of Creep-Fatigue Damage in SUS316 Stainless Steel", Journal of the Japan Society for Non-Destructive Inspection, Vol.48, No.12, pp.853-861 (1999).

[5] H.Liu, M.Saka, I. Komura, H. Sakamoto: "NDE of Three-Dimensional Parallel Multiple Cracks by Means of the DC Potential Drop Technique Based on the Analysis of Crack Interactions", Journal of the Japan Society for Non-Destructive Inspection, Vol.46, No.7, pp.501-510 (1997).

[6] S. Nakanishi, T. Suzuki, Y. Nakasone: "NDE of High-temperature Low Cycle Fatigue Cracks in SUS316L by DC Potential Difference Method using Four-point Probes", Proceedings of the 63rd JSMS Annual Meetings, No.733(2014).

[7] S. Nakanishi, T. Suzuki, Y. Nakasone: " Variation of 4-point probe DC potential difference caused by growth of multiple-site small cracks in fatigue of SUS316L steel at 873K in air', Proceedings of the 2014Annual Meeting of the JSME/MMD, No.14-3, OS2122(2014).